JOURNAL OF APPLIED ELECTROCHEMISTRY 7 (1977) 239–245

The redox mechanism of the chelate-catalysed oxygen cathode

F. BECK

Main Laboratory of BASF Aktiengesellschaft, D 67 Ludwigshafen, Germany

Received 20 September 1976

The electro-reduction of oxygen is effectively catalysed by metal chelates of the N4-type. The mechanism of this process has been found to be a modified 'redox catalysis'. O_2 molecules and the products of their reaction, at least up to H_2O_2, remain strongly co-ordinated to the central metal ion of the chelates XMe^{II}. The potential-determining step, which regenerates the reduced form, is the following:

$$(XMe^{III}...O_2H)^+ + H^+ + 2\,e \longrightarrow XMe^{II} + H_2O_2.$$

H_2O_2 is further decomposed via the catalase action of the electrocatalyst.

The mechanism is confirmed by experimental results with iron phthalocyanine (FePc) and cobalt-dibenzotetraazaannulene (CoTAA) as a O_2-slurry electrode at various O_2 pressures. The latter shows anodic reaction-limited currents, which seem to involve also oxygen-containing intermediates. The implication of the presented mechanism in regard to other electrochemical processes is discussed briefly.

1. Introduction

As well as with metals of the platinum group and silver, effective electrocatalysis at the oxygen cathode is known to proceed with some iron- and cobalt-chelates of the N4-type*. The most promising materials have been shown to be phthalocyanines [1, 2], dibenzotetraazaannulenes [3, 4] and tetraphenylporphyrines [5, 6]. A comprehensive review on this field which is of great practical interest for fuel cells and metal air batteries, has been published recently [7].

As in natural hemin, the co-ordination of the O_2 molecule takes place on top of the central ion of the planar metal-chelates. Besides O_2, solvent molecules or anions such as CN^- can act as the sixth ligand [21]. With O_2, a side-on [5, 6] as well as an edge-on [8] configuration has been discussed. In the case of phthalocyanines, a reversible sorption without splitting of the O_2-molecule has been confirmed experimentally [9]. With solubilized phthalocyanines, O_2-bridged dimers have been found [28]. The nature of this co-ordinative bond, which is of great importance in regard to the kinetics of the reduction steps, will be influenced by the following:

(a) The central ion, which must be capable of providing one electron. Thus, the activities of Fe^{2+} and Co^{2+} are in all cases superior to those of Ni^{2+}, Cu^{2+} and Zn^{2+} [1–8].

(b) The hetero-atoms, where the central ion is attached. For iron complexes the following sequence turns out to be valid [7].

$$N_4 > N_2O_2 > N_2S_2 > O_4, S_4.$$

(c) The nature of the substrate (carrier), which acts as the fifth co-ordination site [2, 7].

The overall reaction to be considered involves four electrons and four protons, and thus it is very complex. The uptake of the first electron (in acid solution) and the further reduction of hydrogen peroxide, which is known to be a characteristic intermediate [10], are slow steps and must be accelerated by electrocatalysis [11, 12]: c means chemical step and e electrochemical step.

$$\begin{array}{l} O_2 \xrightarrow{e} O_2^- \xrightarrow{cec} H_2O_2 \xrightarrow{ecec} 2H_2O \\ \qquad\qquad\qquad\quad \Big\downarrow \text{cat.} \\ \qquad\qquad\qquad\quad H_2O + 1/2\,O_2. \end{array} \qquad (1)$$

H_2O_2 can be removed in parallel by catalytic

* N4 means that the metal ions are linked to four nitrogen atoms of the chelate-forming compound.

decomposition; the catalase activity of iron phthalocyanine (FePc) has been established for a long time [21]. However, catalase activity and overall electrocatalytic activity generally do not run in parallel [3, 4, 7]. This indicates the importance of the promotion of the first electronation step. According to a mechanism previously published [3, 4], which was named 'redox catalysis', the metal chelate XMe was chemically oxidized by oxygen

$$XMe + 1/4\ O_2 + H^+ \longrightarrow (XMe)^+ + 1/2\ H_2O. \quad (2)$$

In a succeeding electrochemical step, the oxidized metal-chelate $(XMe)^+$ was reduced again:

$$(XMe)^+ + e \longrightarrow XMe. \quad (3)$$

However, this simplified mechanism is not in full accordance with all the experimental findings, as was discussed in [7]. The aim of the present work is to present an improved mechanism which is free of these difficulties.

2. Experimental

The measurements have been performed with cobalt-dibenzotetraazaannulene (CoTAA) [13], which has been found to be the most active metal chelate [3–5]. The pigment was purified by vacuum sublimation. 100 mg of the pigment were dissolved under Ar in 100 g 97% H_2SO_4. 100 mg undensified acetylenic black were dispersed in addition. The mixture was introduced dropwise into 955 ml of 1·33 M H_2SO_4 to make up a slurry electrode CoTAA/C in 1 litre of 4·5 N H_2SO_4. The pigment should be precipitated at least partially on to the carbon. The current–voltage curves were measured with an Au/Pt (90/10) mesh feeder electrode ($A = 4{\cdot}5\ cm^2$) polarized against a platinum counter-electrode (separated by a sintered glass disc) under vigorous stirring. The influence of the characteristic parameters on the performance of this special type of slurry electrode will be published [27].

Nitrogen or 10–100% oxygen was bubbled through the solution. The potential of the slurry electrode was measured versus a 1 N HgI–sulphate reference electrode. All curves are plotted against the standard hydrogen electrode U_H. The temperature was 25° C. Further experimental details have been previously published [3].

3. Results

3.1. *Cyclic current–voltage curves with various O_2-partial pressures*

Each of the O_2 partial pressures, varying between 0 and 1 bar, were maintained 30 min before the measurement of the current–voltage curve. The potential range was $U_H = 1–0$ V, the sweep rate 300 mV min^{-1}. The results are given in Figs. 1 and 2. Measurements in a restricted potential range of 1·0–0·6 V and with 50 mV min^{-1} are represented in Fig. 3. The starting potential throughout was 1·0 V.

The rest potential is about 0·8 V. At more positive potentials, a reaction-limited current $i_{a,\,lim}$ is observed. The cathodic currents correspond to oxygen reduction or chelate reduction. Below 0·4 V, oxygen is reduced with a diffusion-limited current $i_{c,\,lim}$. In Figs. 1 and 2, a superimposed cathodic peak at 0·44–0·49 V and an anodic peak at 0·64 V are observed. Correction of the cathodic

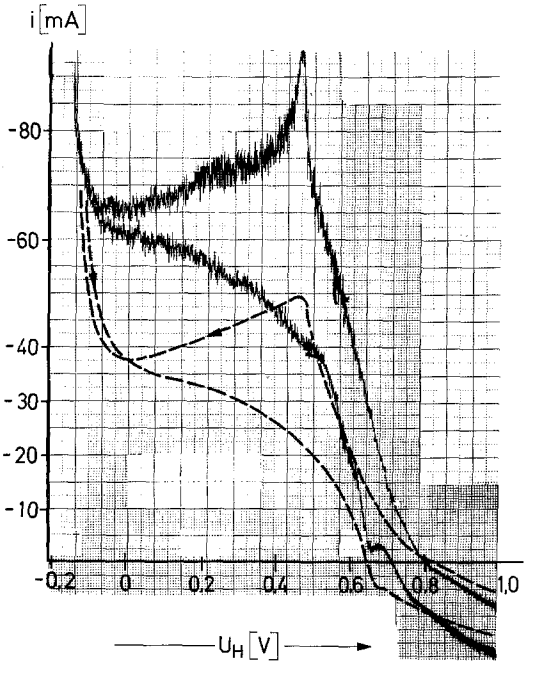

Fig. 1. Potentiodynamic current–voltage curves for the reduction of oxygen at a CoTAA catalysed slurry electrode:
potential range $U_H = 1{\cdot}0 \div -0{\cdot}2$ V;
sweep rate 300 mV min^{-1}.
——— $p_{O_2} = 1$ bar (original curve);
– – – – $p_{O_2} = 0{\cdot}5$ bar (50% N_2).

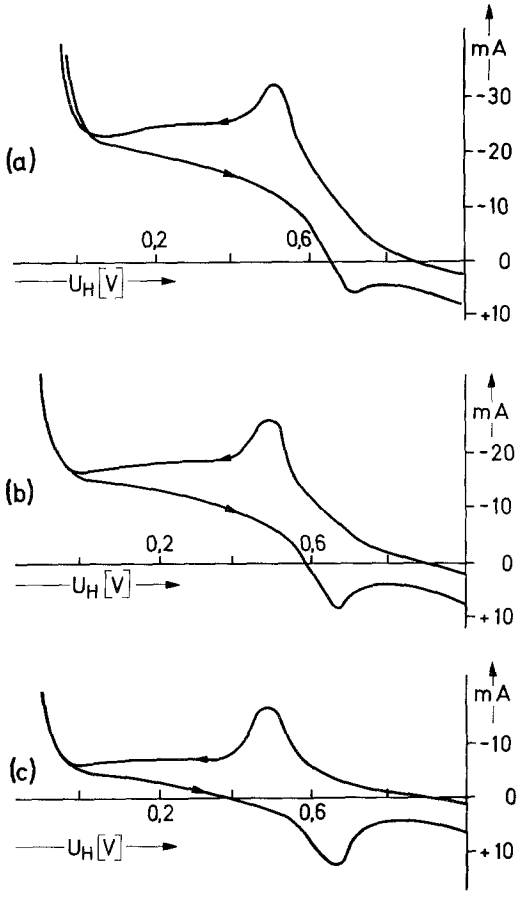

Fig. 2. Potentiodynamic current–voltage curves as in Fig. 1, but (a) p_{O_2} = 0·2 bar (80% N_2); (b) p_{O_2} = 0·1 bar (90% N_2); (c) p_{O_2} = 0 bar (100% N_2)

currents with the corresponding currents under N_2 leads to the following relationships

$$i_{c,0\cdot63} \sim p_{O_2} \qquad (\text{at } U_H = 0\cdot63 \text{ V})$$

$$i_{c,\lim} \sim p_{O_2}.$$

Contrary to the first curves with deep cathodic polarization, the curves in Fig. 3 with an inversion potential at 0·6 V exhibit no hysteresis. $i_{a,\lim}$ is a reaction-limited current, which is constant up to oxygen evolution at U_H = 1·8 V. It decreases with decreasing p_{O_2}. No simple relationship between these two quantities exists.

3.2. *Time-dependent changes of U/i-curves*

(a) With cathodic polarization (p_{O_2} = 1 bar), the current (at U_H = 600 mV) decreases continuously after some hours [3]. Repetition of the current–voltage curves according to Fig. 1, leads to a corresponding decrease of the cathodic currents, but $i_{a,\lim}$ has not changed. The peak at 0·44 V has disappeared.

(b) Stirring under O_2 at the rest potential (0·8 V) and periodical measurement of the current–voltage curves leads to the results represented in Fig. 4. The cathodic branch remains unchanged, the anodic $i_{a,\lim}$ decreases with time.

(c) The cyclic curve under nitrogen exhibits redox peaks at 0·52 and 0·64 V [3], cf. Fig. 2c. The primary curve shows an anodic peak at 0·75 V

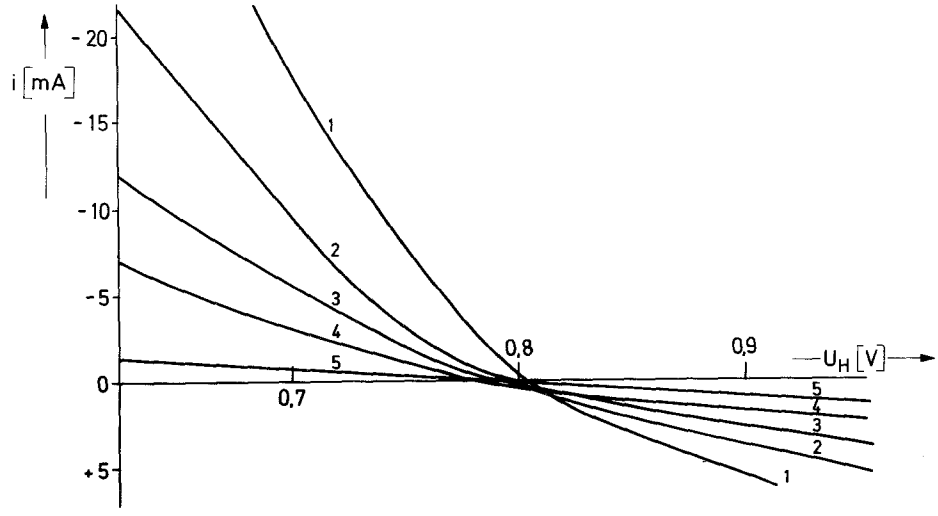

Fig. 3. Potentiodynamic current–voltage curves as in Fig. 1, but potential range U_H = 1·0 ÷ 0·6 V, sweep rate 50 mV min^{-1}, 1–5 at p_{O_2} = 1–0·5–0·2–0·1–0 bar respectively.

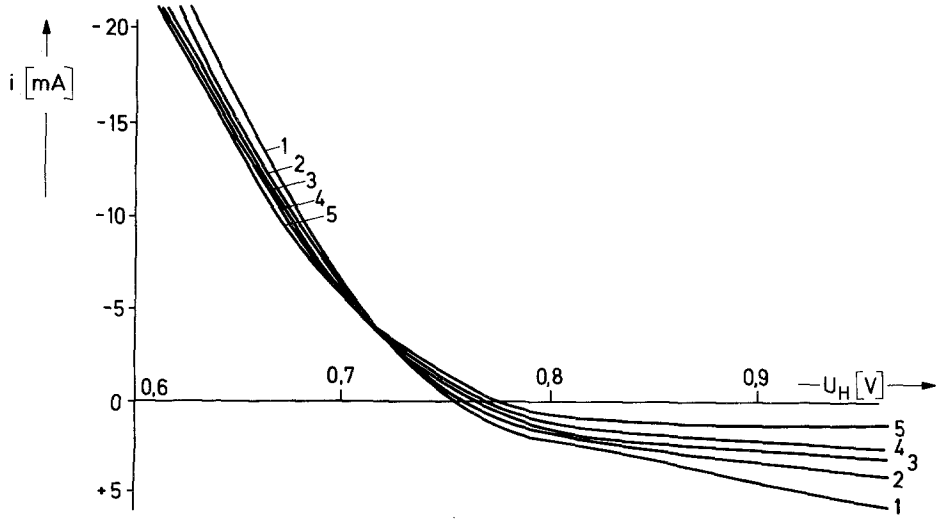

Fig. 4. Potentiodynamic current–voltage curves as in Fig. 1, but potential range $U_H = 1{\cdot}0 \div 0{\cdot}6$ V; sweep rate 50 mV min^{-1}. The curves have been measured at $p_{O_2} = 1$ bar and after continuous stirring under oxygen for 1–5 at 0–0·5–2–4–7·5 h respectively with a rest potential. $U_H = 0{\cdot}76$–0·76–0·765–0·77–0·775.

in addition; this peak is irreversibly removed upon cycling [7].

4. Discussion

4.1. *Reversible redox peaks*

CoTAA shows a pair of reversible redox peaks at $U_H = 0{\cdot}64/0{\cdot}52$ V. These have been reported upon previously [3, 4, 7]. Two interpretations are possible. One involves an oxidation of the ring system to form the di-cation, which is stabilized in the aromatic state with 14 π electrons [3]:

$$Co^{II}\text{–}TAA \rightleftharpoons [Co^{II}\text{–}TAA]^{2+} + 2\,e. \quad (4)$$

The other involves a change in valency of the central ion:

$$Co^{II}\text{–}TAA \rightleftharpoons (Co^{III}\text{–}TAA)^{+} + e. \quad (5)$$

The first mechanism is the most likely. However, it is not possible to choose between them on the basis of our results with the powder electrode [3] or with the slurry electrode reported in this work. The charges under the peaks in Fig. 2 correspond to very low conversions of about 1% according to Equation 4. Jahnke [7] derives, from measurements with 'painted on' electrodes $z = 1$ (according to Equation 4). On the other hand, voltametric measurements in concentrated sulphuric acid showed only a two-electron oxidation [4].

4.2. *Modified mechanism of redox catalysis*

The steady-state reduction of oxygen occurs at potentials which are essentially more positive than the oxidation peak corresponding to processes 4 or 5, as is shown in Fig. 1. The same is true for FePc, where oxygen is reduced at potentials anodic to the reduction peak at 0·66 V [2, 3, 7]. From this one must conclude that a mechanism according to Equation 2 and Equation 3, which we call path A, cannot be valid exclusively.

This discrepancy can be overcome, if a parallel path B, in which an oxygen-containing metal-chelate is reduced in the electrochemical step is assumed

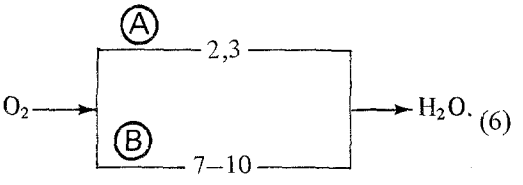

(6)

The following steps must be taken into consideration:

$$XMe^{II} + O_2 \rightleftharpoons (X\overset{\delta+}{M}e\ldots\overset{\delta-}{O}_2) \quad (7)$$

$$(X\overset{\delta+}{M}e\ldots\overset{\delta-}{O}_2) + H^{+} \longrightarrow (XMe^{III}\ldots O_2H)^{+} \quad (8)$$

$$(XMe^{III}\ldots O_2H)^{+} + H^{+} + 2\,e \longrightarrow XMe + H_2O_2 \quad (9)$$

$$H_2O_2 \xrightarrow[\text{(catalase action)}]{\text{XMe}} H_2O + 1/2\ O_2. \quad (10)$$

The metal chelate XMe in the reduced state, which will be called Red, may be co-ordinated with water (XMe... OH_2). According to this mechanism, O_2 molecules are co-ordinated primarily at the sixth co-ordination site of the metal chelate by the equilibrium 7. This primary step has also been proposed for the action of MeX as an oxidation catalyst [29]. The following chemical reaction 8 involves the proton-assisted chemical reduction of the O_2 molecule to yield the chelate with the oxidized central ion, co-ordinated with a radical HO_2. This species is called Ox in the following. In the potential-determining step 9, Ox is electrochemically reduced with the assistance of one proton to yield 'Red' and H_2O_2. The latter decomposes catalytically according to Equation 10.

The rate of formation of Ox is given by:

$$\frac{d[Ox]}{dt} = k_c K p_{O_2} [H^+][Red]. \quad (11)$$

All symbols in brackets mean surface concentrations. K is the equilibrium constant in 7. The intermediate Ox is consumed by the electrochemical step 9, the rate of which is given at higher overpotentials by:

$$\frac{d[Ox]}{dt} = k_e \cdot [H^+][Ox] \exp\left(\frac{2\beta\eta F}{RT}\right) \quad (12)$$

where β is the transfer coefficient and k_e is the electrochemical rate constant.

In the steady state, both rates are identical, and the following ratio of concentrations of redox components is derived:

$$\frac{[Red]}{[Ox]} = \frac{k_e \exp\left(\frac{2\beta\eta F}{RT}\right)}{k_c K p_{O_2}}. \quad (13)$$

The ratio turns out to be independent of pH. For a given system, the relative amount of [Red] increases with increasing overvoltage (at constant oxygen pressure). This is shown in the schematic representation of Fig. 5. The redox potentials of FePc and CoTAA and the equilibrium potentials of the H_2O_2/O_2- and H_2O/O_2-electrodes are indicated, together with the current–voltage curves at C-, C/CoTAA- and Pt-electrodes at pH O. The catalysed curves are situated in the neighbourhood of the O_2/H_2O_2 potential and run in parallel to the redox curves, as is indicated by Equation 13.

With constant η, [Ox] increases with increasing k_c, K and p_{O_2}, i.e. with the increasing reversibility

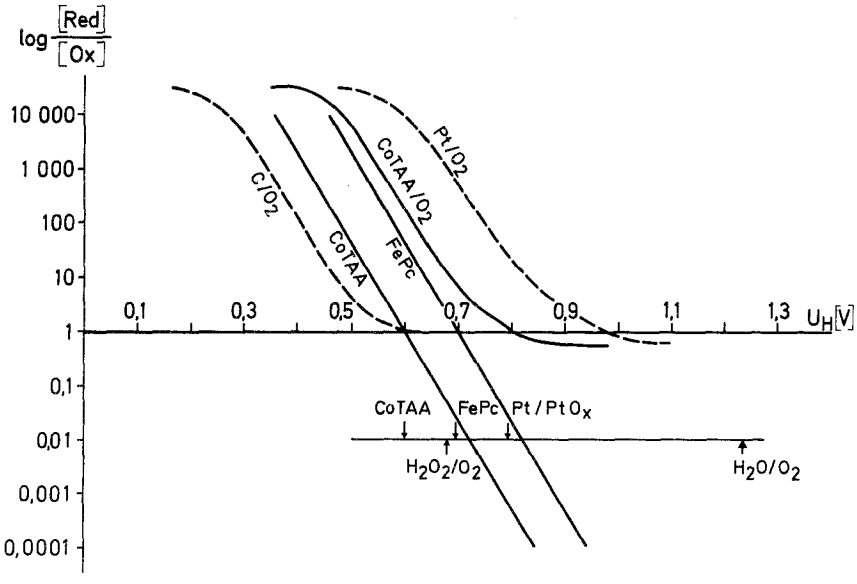

Fig. 5. Schematic representation of current–voltage curves for oxygen reduction at platinum-, CoTAA- and carbon-electrodes, of the dependence of the redox potentials on the ratio [Red]/[Ox] and of various oxygen- and redox standard potentials.

of the reactions 7 and 8. Thus, with active catalysts, the relative concentration of this cationic intermediate increases. This means that there is a higher probability that they will dissolve from the surface [3, 4]. The observation, that the activity and the stability of the catalyst run in opposite directions, would be explained by this mechanism.

With the assumption that Equations 7 and 8 are in equilibrium, the following current–voltage relationship follows from Equation 12:

$$i = 2Fk_eK'p_{O_2}[H^+]^2[\text{Red}]\exp\left(\frac{2\beta\eta F}{RT}\right). \qquad (14)$$

In most cases, [Red] ≫ [Ox] (cf. Fig. 5); thus [Red] ≈ $[MeX]_0$, where $[MeX]_0$ is the total surface concentration of the metal chelate. Under this condition, $j_\eta \sim p_{O_2}$ follows from Equation 14; this agrees with the experimental results. With small p_{O_2}, deviations are to be expected.

The modified mechanism is further confirmed by the following experimental facts:

(a) The current–voltage curves show Tafel slopes of 60 mV dec^{-1} [7].

(b) Equilibrium potentials depend on pH (30 mV pH^{-1}), as is expected from Equation 9. On the other hand, the uncatalysed O_2-electrode has an equilibrium potential, which depends on pH (60 mV pH^{-1}). Thus, the decrease of the difference between the potential and the theoretical potential by about 0·3 V in alkaline solution [3, 27] is satisfactorily explained.

(c) The central ion, chelate and carrier, whose effects have been mentioned in the introduction, influence the electron density at the point of co-ordination, thus influencing all steps of the reaction.

(d) The opposed behaviour of the activity and the stability of the electrocatalyst, formerly correlated with the cationic nature of the intermediate [3, 4] follows also from the new mechanism, as was pointed out above.

On the basis of the published oxidation potentials [14], Randin [15] stated that inactive NiPc and CuPc should exhibit the most positive potentials. However, according to our mechanism, no discrepancy exists. The potentials of the inactive catalysts are too positive and thus step 8 would become too slow.

At least with CoTAA, two reaction paths A and B according to scheme 6, must be considered, otherwise the superimposed redox peaks (cf. Figs. 1 and 2) would not be understandable. At an electrode working for a long time, path A seems to become negligible.

4.3. *Meaning of the anodic current $i_{a,\,lim}$*

The electrochemical oxidation, which is involved in the anodic limiting current, seems to originate from an oxygen-containing species as well. The question, is this intermediate identical with $(XMe\ldots O_2H)^+$, or is it another intermediate 'Ox_1', must remain open. In every case, the oxidation proceeds irreversibly according to

$$XMe + yO_2 + zH^+ \xrightarrow{c} (XMe\ldots yO_2H_z)^{z+} \begin{cases} \xrightarrow{-e} P. \\ \xrightarrow{O_2} \end{cases} \qquad (15)$$

The rate is limited by the chemical step c. The experimental results in Section 3.2 indicate the following:

Ox_1 is present at a working O_2-cathode in a steady-state concentration.

The chemical oxidation proceeds at the rest potential (U_H = 0·8 V).

The rate of step c decreases with decreasing p_{O_2} according to Equation 15.

Under N_2, a 'stock' of Ox_1 is consumed in an irreversible oxidation [7].

Some information on the irreversible chemical or electrochemical oxidation of CoTAA is available from the literature [3, 7, 13]. The structure of the product of oxidation is not known. The electrocatalytic activity for oxygen reduction is substantially diminished [3]. The increase of $i_{a,\,lim}$ after strong cathodic polarization (cf. Figs. 1 and 2) cannot be interpreted by this mechanism.

4.4. *Meaning of the rest potential*

According to the proposed mechanism, the rest potential of the CoTAA/O_2-electrode is a mixed potential. The anodic partial current is given by Reaction 15, the cathodic one by the sequence 6–9.

4.5. *Other examples of redox catalysis*

The electrochemical behaviour of chelate-catalysed oxygen cathodes is satisfactorily understood with the aid of our modified mechanism. Mechanistic suggestions from other authors differ from ours in that at least one of the electrochemical steps occur with the unco-ordinated oxygen or its reduction products [8, 9, 16, 17]. The present mechanism seems to be applicable in some other cases. For example, it constitutes one mechanistic possibility for the oxygen cathode catalysed with platinum metals [18, 19] or with silver:

$$Pt + 1/2\ O_2 + H_2O \xrightarrow{e} Pt(OH)_2. \quad (16)$$

$$Pt(OH)_2 + 2\ e \xrightarrow{e} Pt + 2\ OH^-. \quad (17)$$

This mechanism is strongly supported by the fact that O_2 and PtO_x are reduced at very similar potentials [11, 12], cf. Fig. 5.

Breiter [20] has observed similar anodic reaction-limited currents with platinum metals. Moreover, a reduction peak on top of the cathodic diffusion-limited current was observed in addition with the relatively stable palladium oxide. An analogous redox-mechanism may be suggested for chlorine evolution on RuO_2-activated titanium electrodes. Ru may change its valency between III and IV.

In organic electrosynthesis, redox mediators play some role [22]. Examples are Sn^{2+} and Cr^{2+} for reductions and Br_2, Co^{3+}, $HCrO_4^-$, Ce^{4+} and Mn^{3+} for oxidations. The redox system, present in small concentrations, establishes a reaction layer in front of the working electrode, from where no intermediate escapes to the counter electrode. Similar conditions are realized in the redox fuel cell [11]. Polarographic measurements of O_2 reduction in the presence of ferrohem [23], catalase [24] or synthetic metal chelates [4, 16] and of H_2O_2 in the presence of Fe^{2+} ions [25] have been interpreted in the terms of redox catalysis.

Another case of some interest is that of the redox reactions which occur at both electrodes of the electrochemical cell, for example Fe^{2+}/Fe^{3+} in secondary batteries, where it acts like an 'electrochemical short circuit' [30] and in electrochemical solar cells [26].

Acknowledgements

The author thanks Dr Hiller, BASF Aktiengesellschaft, for providing purified CoTAA and Mr Böhn and Mr Reitz for their valuable experimental work.

References

[1] R. Jasinski, *Nature* **201** (1964) 1212 and *J. Electrochem. Soc.* **112**, (1965) 526.
[2] H. Jahnke, *Ber. Bunsenges. physik. Chem.* **72** (1968) 1053; H. Jahnke and M. Schönborn, *III. Journées Int. d'Etude des Piles à Combustible, Compt. red. Bruxelles* (1969) 60.
[3] F. Beck, W. Dammert, J. Heiss, H. Hiller and R. Polster, *Z. Naturforsch.* **28a** (1973) 1009.
[4] F. Beck, *Ber. Bunsenges. physik. Chem.* **77** (1973) 355.
[5] H. Alt, H. Binder, W. Lindner and G. Sandstede, *J. Electroanal. Chem.* **31** (1971) 19.
[6] H. Alt, H. Binder and G. Sandstede, *J. Catal.* **28** (1973) 8.
[7] H. Jahnke, M. Schönborn and G. Zimmermann, *Topics Current Chem.* **61** (1976) 133.
[8] M. Savy, P. Andro, C. Bernard and G. Magner, *Electrochim. Acta* **18** (1973) 191.
[9] J. P. Counter, P. Lenfant and A. K. Vijh, *J. Catal.* **29** (1973) 8.
[10] F. Haber, *Z. anorg. Chem.* **51** (1906) 356.
[11] J. P. Hoare, 'The Electrochemistry of Oxygen', Interscience, New York (1968).
[12] V. N. Bagotskii, L. N. Nekrassow and N. A. Shumilowa, *Russ. Chem. Rev.* **34**, (1965) 717.
[13] H. Hiller, P. Dimroth and H. Pfitzner, *Liebgs Ann. Chem.* **717** (1968) 137.
[14] J. Manassen and A. Bar-Ilan, *J. Catalysis* **17** (1970) 86.
[15] J. P. Randin, *Electrochim. Acta* **19** (1974) 83.
[16] W. Beyer and F. v. Sturm, *Angew. Chem.* **84** (1972) 154.
[17] Chr. Kretschmar and K. Wiesener, *Z. phys. Chem. (Leipzig)* **257** (1976) 39.
[18] D. I. Sawyer and L. V. Interrante, *J. Electroanal. Chem.* **2** (1961) 310
[19] D. I. Sawyer and R. J. Day, *Electrochim. Acta* **8** (1963) 589.
[20] M. W. Breiter, 'Electrochemical Processes in Fuel Cells', Springer, Heidelberg (1969).
[21] H. A. Cook, *J. Chem. Soc.* (Lond.) **1938** (1974) 1761.
[22] M. M. Baizer (Ed.) 'Organic Electrochemistry', M. Dekker, New York (1973).
[23] R. Brdička and K. Wiesener, *Naturwiss.* **31** (1943) 247 and *Coll. Czech. Chem. Comm.* **12** (1947) 39.
[24] J. Koutečky, R. Brdička and V. Hanus, *Coll. Czech. Chem. Comm.* **18** (1953) 611.
[25] I. M. Kolthoff and E. P. Parry, *J. Amer. Chem. Soc.* **73** (1951) 3718.
[26] H. Gerischer and J. Gobrecht, *Ber. Bunsenges. physik. Chem.* **80** (1976) 327.
[27] F. Beck *J. Electroanal. Chem.* (to be published).
[28] D. Vonderschmitt, K. Bernauer and S. Fallab, *Helv. Chim. Acta* **48** (1965) 951
[29] H. Kropf, *Liebigs Ann. Chem* **637** (1960) 73.
[30] E. Willihnganz, *J. Electrochem. Soc.* **100** (1953) 527.